

# A Parallel Sectionalized Restoration Scheme for Resilient Smart Grid Systems

Saeedeh Abbasi, *Student Member, IEEE*, Masoud Barati, *Member, IEEE*, and Gino J. Lim *Member, IEEE*

**Abstract**—A parallel automated resilience-based restoration methodology is presented in the power system to minimize impact due to emergency power outages. In this power restoration process, a black start (BS) unit is assigned to a small region (i.e. a section) on an as-needed basis. A mixed integer nonlinear programming (MINLP) model is developed in order to optimally sectionalize the region of interest all the while maximizing the resiliency in terms of load shedding, restoration time, and network connectivity. For solving this large scale optimization model, a bi-level programming (BLP) approach is proposed. This approach consists of two optimization levels. The sectionalization problem (upper level) is a mixed integer programming (MIP) model and finds the optimal section set. The restoration problem (lower level) is a linear model and determines the DC optimal power flow (DC-OPF) and restoration time for the optimal section set identified in the upper level. We use the pre-emptive method of goal programming to deal with multiple conflicting objectives in the model. Our proposed solution approach outperformed mathematical programming with equilibrium constraints (MPEC) and found near optimal solutions. Numerical results and sensitivity analysis from two case studies (6- and 118 bus IEEE test systems) are further discussed to demonstrate the efficiency of the solution approach.

**Index Terms**—bi-level programming, infrastructure, pre-emptive programming, resilience, robustness, power network restoration, sectionalization.

## NOMENCLATURE

### Notation

$NB$	Number of buses
$NBS$	Number of Black Start units
$NT$	Number of periods under study (24 h)
$ND$	Number of loads
$NL$	Number of transmission lines

### Set

$b / b'$	Index for buses, $b = \{1, \dots, NB\}$
$m$	Index for sections, $m = \{1, \dots, NBS\}$
$t$	Index for time, $t = \{1, \dots, NT\}$
$g$	Index for generators, $g = \{1, \dots, NBS\}$
$d$	Index for demand loads, $d = \{1, \dots, ND\}$
$l$	Index for transmission lines, $l = \{1, \dots, NL\}$
$k$	Index for iterations

### Parameters

$w_b, w_d$	Cost of delay in restoration of bus $b$ /demand load $d$ (\$/hr)
$VOLL$	Value of lost load (\$/MWh)
$c_g$	Cost of generation in unit $g$ (\$/MWh)
$U_l$	Availability of line $l$
$P_{gt, \max}, P_{gt, \min}$	Maximum and minimum limits of generation dispatch unit $g$ , at time $t$
$PL_{l, \max}$	Power line capacity of line $l$

$UR_g/DR_g$	Ramp up/down rate of unit $g$
$CT_t$	Auxiliary current time equal to $t$ at time $t$
$x_l$	Reactance of line $l$
$D$	Load demand matrix ( $ND \times NT$ )
$KG$	Incident matrix of units ( $NB \times NBS$ )
$KL$	Incident matrix of lines ( $NB \times NL$ )
$KD$	Incident matrix of demands ( $NB \times ND$ )
<b>Variables</b>	
$s_{mb}$	Bus indicator $b$ at section $m$ ; equal to 1 if bus $b$ is belonged to section $m$ ; otherwise 0
$LS_{mt}/\tilde{L}S_{dt}$	Total load shedding at section $m$ /load $d$ at time $t$
$P_{gt}$	Generation dispatch of unit $g$ at time $t$
$T_{mb}$	The total restoration time of bus $b$ in section $m$
$\tau_{mb}^b$	The upper bound of $T_{mb}$
$\tau_d^{Load}$	Load pick up time of demand $d$
$T_d$	The total restoration time of demand $d$
$PL_{lt}$	Power flow on line $l$ at time $t$
$\theta_{bt}$	Phase angle of bus $b$ at time $t$
$T_{dt}$	Restoration indicator; equal to $CT_t$ when, load shedding of demand $d$ is zero at time $t$ ; otherwise big $M$ ( $=25h \times LS_{dt}$ )
$T$	Total restoration time vector
$PL$	Line real power flow matrix
$P_G$	Unit real power generation matrix
$LS/\tilde{L}S$	Load shedding matrix of sections/Load buses

## I. INTRODUCTION

Extreme events can cause multiple faults simultaneously, which may result in cascading outages in power systems [1]. Disasters such as hurricanes can inflict significant damage to exposed power transmission lines installed in wide open areas [2]. Blackouts that have recently occurred across the globe have inspired new research to not only prevent failures before they happen, but to take the right precautions to undertake a power system restoration [3]–[12].

A *resilient* power system has the ability to mitigate ensuing negative impacts in the presence of natural disasters. Multiple definitions for a resilient system have been developed in the literature. For example, UK Energy Resource Center stated that “a resilient energy system can speedily recover from shocks and can provide alternative means of satisfying energy service needs in the event of changed external circumstances” [13]. The National Infrastructure Advisory Council (NIAC) described the inherent features of resiliency as *robustness*, *resourcefulness*, *rapid recovery* and *adaptability*. Per NIAC [14], robustness is the ability of the system to withstand low probability, high impact events, while resourcefulness is defined as the system’s capability to effectively manage a disaster as it happens. Rapid recovery is a criterion to assess the system recovery to the normal state in a short time, and adaptability is the competence of the system to mitigate future losses by learning from past similar events. These are the main

S. Abbasi and G. J. Lim are with the Department of Industrial Engineering, University of Houston, TX 77204 USA (e-mail: {sabbasi5, ginolim}@uh.edu). M. Barati is with the Department of Electrical and Computer Engineering, Louisiana State University, Baton Rouge, LA 70803 USA (e-mail: mbarati@lsu.edu).

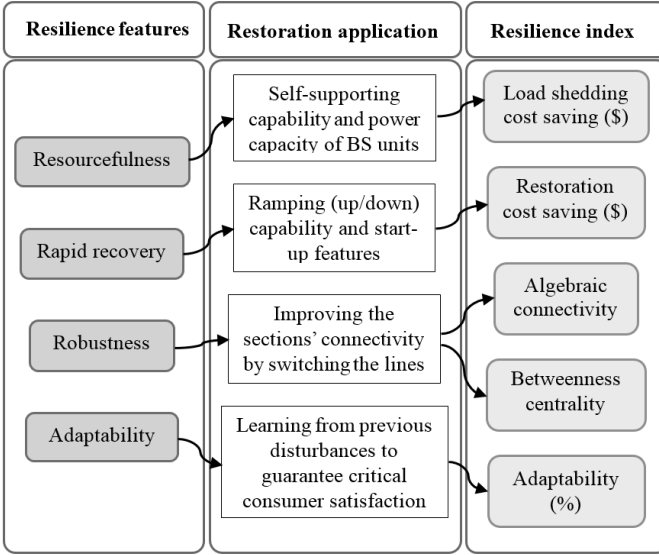


Fig. 1. Resilience Main Features

features considered in the proposed power grid restoration method in this paper as highlighted in Fig. 1. Investigating the resilience of a power system, Fig. 2 shows a typical resilience curve corresponding to an extreme event. The system's state axis in Fig. 2 represents the state of a power grid in different operating states including normal, alert, and restorative [16]. The system operating state includes event progress  $[t_0, t_{pe}]$ , post-event degraded state  $[t_{pe}, t_r]$ , restorative state  $[t_r, t_{pr}]$ , post-restoration or alert state  $[t_{pr}, t_{ir}]$ , and post-restoration activities  $[t_{ir}, t_{pir}]$ . This paper focuses on restorative actions during the time period  $t_{pe}$  to  $t_{pr}$  following an imposed disturbance to recover the most critical load with the highest priority in the power transmission system.

To plan a more resilient system against undesirable events, one can appeal to the level of resiliency of a power system. Several publications in the past have proposed qualitative measures [5], however, very few researchers have resorted to quantitative approaches [6], [17]. A resilience metric can be defined based on performance function of the system [18], [19], or designed through a probabilistic resilience assessment relied on the Poisson distribution for disaster occurrence [20]. One of the aims of this paper is to propose a quantitative approach to measure the resiliency of power system networks. Following the guidelines outlined in NIAC [14], five resilience indexes are parametrized based on four different resiliency features, as explained in Fig. 1, along with possible applications in power system restoration. These indexes are explained in detail in Section II. The restoration process is influenced by network topology and energy resources. From the network topology perspective, the line switching capability enables the network to restore connectivity, which can be measured according to graph theory. Hereby, the connectivity is quantified by *algebraic connectivity* and *betweenness centrality*. These metrics guarantee the robustness of the resilient network [21]–[23]. In the energy resources front, the system restoration must begin with pre-assigned generation units with the self-starting capability. These units are often referred to as black-starts (BS) and are able to provide a rapid recovery. The primary purpose

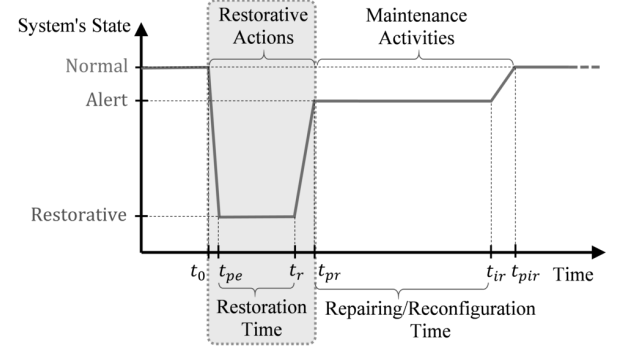


Fig. 2. Power System States Under Disruption Risk [15]

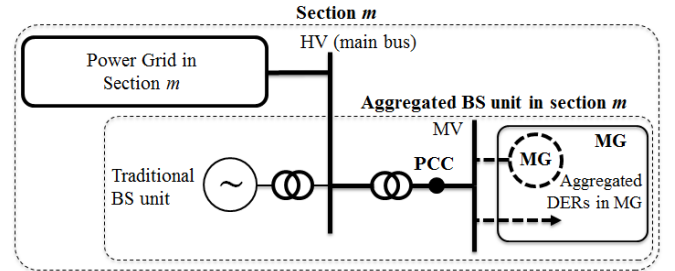


Fig. 3. Aggregated Black-Start Generation Unit

of BS units is to generate initial power for non-black start (NBS) units that are responsible for generating the necessary power in the network.

The principal focus of this paper is on the BS units, which are imposed as the main resources of power generation in response to network demands during the restoration process. Accordingly, aggregated BS (ABS) generating units are considered as self-supported units to improve the rapid recovery, and resourcefulness resilience features [24]. Figure 3 shows the ABS unit including microgrids (MGs) with aggregated distributed energy resources (DERs) in Medium Voltage (MV) level and traditional BS unit in High Voltage (HV) level. The application of DERs in ABS units has two advantages: 1) Larger capacity of BS unit: ABS units have much higher capacities to energize each island. In the other word, the main assumption of this paper is to use the capability of DER units to increase the level of resourcefulness capability of BS units in the restoration process. 2) Lower load pick up time: The DERs units including renewable energy resources and energy storage systems (ESS) have a minimum start up and load pick up times. The ABS units have faster cranking power process in comparing to NBS units. Therefore, this capability affects the rapid recovery feature of resiliency. Nevertheless, the proposed model in Section III can be easily modified to encompass the NBS units.

Two common strategies for power system restoration are “build-up” and “build-down” [25]. Build-up is preferable in restoring large scale networks due to its faster speed [26]. Hence, the proposed restoration model in this paper focuses on the build-up approach, where the entire system is set up from small individual grid sections. The restoration of sections through a sectionalization approach is called “Parallel Power System Restoration” (PPSR) [25], [27], [28]. This study

conducts a power grid restoration through the PPSR (build-up) approach and will end up with the restored sections.

A power grid sectionalization is one of the restoration's challenges as dealing with a large-scale network. Due to the nature of networks, most of the proposed methods come from graph theory concepts [27]. Heuristics approaches such as genetic algorithm and simulated annealing are popular in restoration planning [29], [30]. Generating a set of the possible restoration plan and checking the feasibility and optimality of them is a common approach in this category [31]. The mathematical modeling is another approach in the literature to find the optimal restoration plan which is merged with the objectives of a build-up restoration process [28], [32].

The main purpose of the build-up restoration process is to restore the majority of transmission lines and loads via sectionalization. Several optimization-based restoration approaches have been reported in designing an appropriate grid sectionalization in the literature. For example, minimizing total *electrical distance* is used in the power system sectionalization [33] while minimizing *load shedding* is also used to find the optimal strategy [25], [34]. Minimizing *restoration time* was also proposed by Liu et.al [28], in which a "Judgment" matrix,  $\mathbf{J} = (\mathbf{S} \oplus (\mathbf{S} \wedge \mathbf{S}\mathbf{A})) \cdot \mathbf{S}^T$ , was defined to ensure that each section was fully connected. A drawback of this approach, however, is in implementation of the Judgment matrix  $\mathbf{J}$  into an optimization model. The resulting mixed integer nonlinear programming (MINLP) model is not easy to solve for a realistic size of the problem. To address this issue, a set of linear constraints are introduced as an alternative to the judgment matrix  $\mathbf{J}$ .

Furthermore, a BLP approach is used to improve the computational efficiency. As a result the restoration problem is divided into two separate optimization problems: sectionalization and energizing. In summary, this paper brings the following three contributions to the literature:

- 1) Resilience of power system networks is quantified to facilitate the restoration process. The proposed resilience indexes measure resourcefulness, robustness, rapid recovery, and adaptability of a power grid.
- 2) We proposed a linear approach to ensure connectivity of networks in the sectionalization process. Our approach significantly reduces computational complexity compared with the nonlinear approach, and it improves the solution quality compared to existing heuristic approaches.
- 3) Two efficient solution methodologies are developed to solve the proposed bi-level restoration model.

The rest of the paper is organized as follows: Section II describes the resilience quantification and Section III presents the proposed resilience-based mathematical model based on BLP. The case studies are presented and analyzed in Section V and the conclusion of the paper is given in Section VI.

## II. RESILIENCE QUANTIFICATION

To quantify the resilience of a power system network, vector  $\mathfrak{R}$  is introduced that contains five resilience indexes:

$$\mathfrak{R} = [\Delta C_{LS}^R, \Delta C_T^R, \lambda_{AL}, \xi_{BTW}, \Pi^R]. \quad (1)$$

1) *Load shedding cost savings* ( $\Delta C_{LS}^R$ ) is the total cost savings (\$) by a load shedding prevention for all sections over a planning time horizon ( $NT$ ):

$$\Delta C_{LS}^R = VOLL \cdot (\mathbf{D} - \mathbf{L}\mathbf{S}) \quad (2)$$

This index reflects the availability of the resources in providing the demands (resourcefulness). It is determined in the energizing level of the model that will be explained in Section III.

2) *Restoration cost savings* ( $\Delta C_T^R$ ) is a product of consumer outage rate  $\mathbf{w}$  (\$/hr) and the difference between  $NT$  and the actual time  $\mathbf{T} = [T_d]_{ND \times 1}$  spent to restore the system.

$$\Delta C_T^R = \mathbf{w}^T \cdot (NT \cdot \mathbf{1} - \mathbf{T}), \quad (3)$$

Hence, a faster restoration time corresponds to a higher  $\Delta C_T^R$  (rapid recovery).

3) *Weighted algebraic connectivity* ( $\lambda_{AL}$ ) is a spectral graph index that indicates the robustness of the network topology [22]. The algebraic connectivity is the second smallest eigenvalue of a network's *Laplacian matrix* [21]. Here, a grid bus can be viewed as a node and a transmission line as an edge in a graph [6]. The algebraic connectivity  $\lambda_m$  is calculated for each section  $m = \{1, \dots, NBS\}$ , and the algebraic connectivity of the whole network is calculated as follows:

$$\lambda_{AL} = \frac{1}{NB} \sum_{b=1}^{NB} \sum_{m=1}^{NBS} s_{bm} \cdot \lambda_m \quad (4)$$

4) *Weighted betweenness centrality* ( $\xi_{BTW}$ ) is defined as

$$\xi_{BTW} = \frac{1}{\sum_{d=1}^{ND} w_d} \left( \sum_{d=1}^{ND} w_d \sum_{b=1}^{NB} KD_{bd} \cdot \xi_b \right) \quad (5)$$

where, betweenness centrality  $\xi_b$  is evaluated for each bus  $b = \{1, \dots, NB\}$ ;  $\xi_b$  is the fraction of the total lengths of all shortest paths passing through a specific node and the total lengths of all shortest paths between all node-pairs in a graph [6], [35].

5) *Adaptability index* ( $\Pi^R$ ) is a function of  $\Delta C_{LS}^R$  and  $\Delta C_T^R$  and it is defined as follows:

$$\begin{aligned} \Pi^R &= \alpha \left( \Delta C_{LS}^{R,*} - \Delta C_{LS}^{R,o} \right) / \Delta C_{LS}^{R,o} \\ &+ (1 - \alpha) \left( \Delta C_T^{R,*} - \Delta C_T^{R,o} \right) / \Delta C_T^{R,o} \end{aligned} \quad (6)$$

Here,  $\Delta C_{LS}^{R,*}$ ,  $\Delta C_{LS}^{R,o}$ ,  $\Delta C_T^{R,*}$ , and  $\Delta C_T^{R,o}$  are respectively the optimal and initial values of  $\Delta C_{LS}^R$  and  $\Delta C_T^R$ . Parameter  $\alpha \in [0, 1]$  is given by a decision maker based on his/her preference.

All these indexes are defined in such a way that a higher value reflects better performance. Hence, we optimize the proposed resilience vector  $\mathfrak{R}$  in the following order. First, two indexes ( $\Delta C_{LS}^R, \Delta C_T^R$ ) are optimized in a resilience-based model (7) described in Section III. Next,  $\lambda_{AL}$ , and  $\xi_{BTW}$  are evaluated at the restoration calculation process. Since the last index ( $\Pi^R$ ) is considered in the first two indexes, it is maximized as a result of optimizing the first two indexes ( $\Delta C_{LS}^R, \Delta C_T^R$ ). These considerations have been elaborated in the proposed optimization model in the following section.

## III. MODEL DESCRIPTION

The goal of the proposed resilience-based model is to optimize the first two resilience indexes ( $\Delta C_{LS}^R, \Delta C_T^R$ ). This can be achieved by minimizing the load shedding cost and the

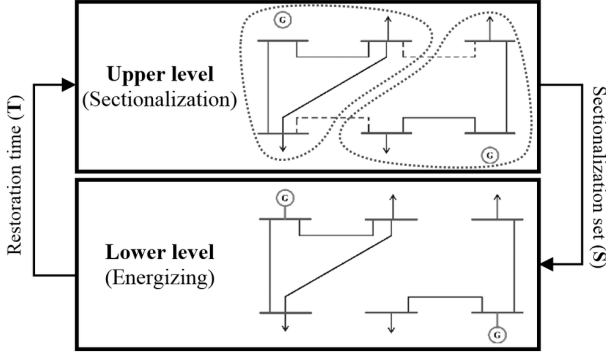


Fig. 4. Bi-level programming

cost of restoration time in the objective function. Additionally, the power generation cost term is added to the objective function to minimize cost of the entire system. Note that all units ( $w$  (\$/hr),  $VOLL$  (\$/MWh), and  $c$  (\$/MWh)) are based on dollars.

where,  $e_i$  is a vector of ones for  $i = 1, 2, 3$ :  $e_1 = [1]_{NBS \times 1}$ ,  $e_2 = [1]_{NT \times 1}$ , and  $e_3 = [1]_{NL \times 1}$ . The model is constrained by the physical operation constraints of generation units (7b) and (7c), transmission line flow limitations (7d)-(7f), power flow equations (7g), and a set of novel restoration and sectionalization constraints (7h) and (7i) that show the relationship among the restoration time, sectionalization variables and state variables of the power system. These constraints are presented in detail in the Subsections IV-A1 and IV-A2.

$$\min_{\mathbf{T}, \mathbf{LS}, \mathbf{P}, \mathbf{PL}, \mathbf{S}, \mathbf{U}} \omega^T \mathbf{T} + VOLL \cdot \mathbf{e}_1^T \cdot \mathbf{LS} \cdot \mathbf{e}_2 + \mathbf{c}^T \mathbf{P} \cdot \mathbf{e}_2 \quad (7a)$$

$$s.t. \mathbf{P}_{G,min} \leq \mathbf{P}_G \leq \mathbf{P}_{G,max} \quad (7b)$$

$$- \mathbf{DR} \leq \mathbf{P}_{G,t} - \mathbf{P}_{G,(t-1)} \leq \mathbf{UR}, \forall t \quad (7c)$$

$$|\mathbf{PL} - \text{diag}^{-1}(\mathbf{x}) \cdot \Delta \boldsymbol{\theta}| \leq M \cdot (\mathbf{e}_3 - \mathbf{U}) \cdot \mathbf{e}_2^T \quad (7d)$$

$$|\mathbf{PL}| \leq \mathbf{PL}_{max} \cdot \text{diag}(\mathbf{U}) \quad (7e)$$

$$\boldsymbol{\theta}_{ref} = \mathbf{0} \quad (7f)$$

$$\mathbf{KG} \cdot \mathbf{P}_G + \mathbf{KL} \cdot \mathbf{PL} + \mathbf{KD} \cdot \mathbf{LS} = \mathbf{KD} \cdot \mathbf{D} \quad (7g)$$

$$f_s(\mathbf{LS}, \mathbf{S}, \mathbf{T}) \leq \mathbf{0} \quad (7h)$$

$$f_u(\mathbf{S}, \mathbf{U}) \leq \mathbf{0} \quad (7i)$$

The objective function (7a) and the above-mentioned constraints can be split into two different technical parts: section formation and optimal load restoration. Section formation sectionalizes the grid by assigning the load buses to black start generation units based on the topology of the grid. Optimal load restoration finds the DC-OPF solution for each section which gives the optimal restoration time of each load. In order to implement the decomposition and solve the model, two approaches are proposed: BLP [36] and MPEC methods.

## IV. SOLUTION METHODOLOGY

### A. Bi-level programming

The BLP approach consists of an upper and lower level of the optimization model. The upper level problem is for *grid sectionalization*, while the lower level problem is for optimal load restoration, which is termed *energizing*. Figure 4 shows a basic BLP structure in which  $\mathbf{T}$  is the restoration time and  $\mathbf{S}$  is the sectionalization set. Hereby,  $\mathbf{T}$  is a controlled variable

from lower level and  $\mathbf{S}$  is a controlled variable from the upper level model.

The upper level starts with an initial  $\mathbf{T}^0$  and sends optimal  $\mathbf{S}$  (i.e.,  $\mathbf{S}^*$ ) to the lower level, the lower level optimization model then finds and returns optimal  $\mathbf{T}$  (i.e.,  $\mathbf{T}^*$ ) to the upper level. This process repeats until both of the following stopping criteria are satisfied:

$$\|\mathbf{S}^k - \mathbf{S}^{k-1}\|_2 = 0 \text{ and } \|\mathbf{T}^k - \mathbf{T}^{k-1}\|_2 = 0, \quad (8)$$

where,  $k$  is the iteration counter.

1) *Upper level-sectionalization*: This sectionalization level aims to identify the optimal network's sections for restoration process. The model might be complicated to solve in large scale network application because of non-linear mixed integer constraints (7i) for determining the states of transmission lines  $\mathbf{U}$ . Therefore, to solve it at lower complexity, all transmission line flow constraints in this level are moved to lower level and the load balance equation (7g) is replaced with a set of single load balance constraints at each section.

The sectionalization model minimizes the total cost of restoration time, load shedding, and power generation. The power generation limits and load balance constraints of each section are presented at (9b)-(9c), where  $\mathbf{S} = [s_{mb}]_{NBS \times NB}$  is the sectionalization set and  $s_{mb}$  is equal to one, if bus  $b$  assigned to section  $m$ ; otherwise  $s_{mb}$  is equal to zero.

$$\min_{\mathbf{S}, \mathbf{P}, \mathbf{LS}, \boldsymbol{\tau}} \sum_{m=1}^{NBS} \sum_{b=1}^{NB} w_b \cdot \tau_{mb} + \sum_{m=1}^{NBS} \sum_{b=1}^{NB} VOLL \cdot LS_{mt} + \sum_{t=1}^{NT} \sum_{g=1}^{NBS} C_g \cdot P_{gt} \quad (9a)$$

$$s.t. P_{g,min} \leq P_{gt} \leq P_{g,max}, \forall g, \forall t \quad (9b)$$

$$\mathbf{S} \cdot \mathbf{KG} \cdot \mathbf{P}_G + \mathbf{LS} = \mathbf{S} \cdot \mathbf{KD} \cdot \mathbf{D} \quad (9c)$$

$$\tau_{mb} \geq s_{mb} \cdot T_{mb} + M \cdot (1 - s_{mb}), \forall m, \forall b \quad (9d)$$

$$s_{mb} \leq \sum_{b'=1}^{NB} s_{mb'} \cdot a_{b'b} \quad (9e)$$

$$\mathbf{S}^T \cdot \mathbf{e}_1 = \mathbf{e}_4 \quad (9f)$$

$$\mathbf{S} \cdot \mathbf{e}_4 \geq \mathbf{e}_1 \quad (9g)$$

The first term of (9c) is a product of  $\mathbf{S}$  as a binary matrix and  $\mathbf{P}_G$  as a real matrix variable. This constraint is reformulated to be linear with given Lemma in [37]. In this order, the non-linear term is replaced with matrix  $\mathbf{Q} = [q_{mt}]_{NBS \times NT}$  and following constraints are added to the model:

$$\mathbf{S} \cdot \mathbf{KG} \cdot \mathbf{P}_{G,min} \leq \mathbf{Q} \leq \mathbf{S} \cdot \mathbf{KG} \cdot \mathbf{P}_{G,max} \quad (10)$$

$$(\mathbf{1} - \mathbf{S} \cdot \mathbf{KG}) \cdot \mathbf{P}_{G,min} \leq \mathbf{P}_G - \mathbf{Q} \leq (\mathbf{1} - \mathbf{S} \cdot \mathbf{KG}) \cdot \mathbf{P}_{G,max} \quad (11)$$

In constraint (9d),  $\tau_{mb}$  is an upper bound of restoration time of bus  $b$  in section  $m$ , and  $T_{mb}$  is the restoration time of bus  $b$  in section  $m$ . In this model,  $T_{mb}$  a controlled variable from the lower level comprising of:

$$T_{mb} = T_{mb}^{Load} + \bar{T}_{mb}^{Switch} + \bar{T}_{mb}^{Relay} + \bar{T}_{mb}^{Delay} \quad (12)$$

The first term  $T_{mb}^{Load}$  is dependent on the generators loading time and the order of load recovery in sections that is updated at each iteration. Other terms include the switching operation duration  $\bar{T}_{mb}^{Switch}$ , the relay reconfiguration time duration  $\bar{T}_{mb}^{Relay}$ , and the expected value of uncertain delay  $\bar{T}_{mb}^{Delay}$  caused by operational uncertainties. With the exception of  $T_{mb}^{Load}$ , the time elements in (12) are constant and estimated with Dijkstras algorithm in [28]. In this order, the length of the lines are assumed to represent the restoration time  $T_{mb}$  rather

than the geographical distance. Considering an initial value for  $T_{mb}^{Load}$ , Dijkstras algorithm gives us the shortest path between each bus and each BS unit. The  $T_{mb}^{Load}$  is ideally initiated with zero and it is updated iteratively by the optimal solution of the energizing level model.

Constraints (9e)-(9g) are the sectionalization constraints such that constraint (9e) prevents locating any single bus without connectivity in the sections, where  $\mathbf{A} = [a_{bb'}]_{NB \times NB}$  is the electrical connectivity matrix that is a symmetric binary-matrix with unit off-diagonal elements  $a_{bb'} = 1$  ( $b \neq b'$ ), where there is a link between buses  $b$  and  $b'$ ; otherwise  $a_{bb'}$  is equal to zero. Constraint (9f) ensures the assignment of each bus to exactly one section, and (9g) eliminates empty sections where  $\mathbf{e}_1 = [1]_{NBS \times 1}$  and  $\mathbf{e}_4 = [1]_{NB \times 1}$ .

2) *Lower level-energizing*: The energizing level model attempts to find the optimal restoration time based on the given sectionalization set from the upper level model. To model the power grid, the DC-OPF with DC power flow under system steady state operation is conducted in (13). The DC power flow equation is a linearization of the AC power flow and merges computational simplicity and straightforwardness through a set of linear equations with an acceptable level of accuracy and convergence speed.

There are two sets of generation resources at each section: single ABS generation unit and multiple load shedding (negative load). These resources come with their costs include marginal generation and load shedding costs. Therefore, a scheduling model is required to find the optimal value of power generation and a minimum level of load shedding in each section as considered in first and second terms of (13a), respectively.

Power generation limits and ramping up and down constraints are presented in (13b) and (13c). Transmission line flow equation and its upper and lower limits are given in constraints (13d)-(13e). The angle of reference bus is assumed to be zero (13f). Constraint (13g) is the load balance constraint. During the energizing process, the exact time of getting zero load shedding in a load bus is identified as its load pick up time ( $T_d^{Load}$ ). The constraint (13h) shows the relationship between restoration time and load shedding value.

$$\min_{\mathbf{P}, \mathbf{PL}, \mathbf{LS}, \tau^{Load}} \sum_{t=1}^{NT} \sum_{d=1}^{ND} VOLL \cdot \tilde{L}S_{dt} + \sum_{t=1}^{NT} \sum_{g=1}^{NBS} C_g \cdot P_{gt} - \sum_{d=1}^{ND} \omega_d \cdot \tau_d^{Load} \quad (13a)$$

$$s.t. \quad P_{gt, min} \leq P_{gt} \leq P_{gt, max}, \forall g, \forall t \quad (13b)$$

$$-DR_g \leq P_{gt} - P_{g(t-1)} \leq UR_g, \forall g, \forall t \quad (13c)$$

$$|PL_{lt} - \Delta\theta_{lt}/x_l| \leq M \cdot (1 - U_l), \forall l, \forall t \quad (13d)$$

$$|PL_{lt}| \leq PL_{l, max} \cdot U_l, \forall l, \forall t \quad (13e)$$

$$\theta_{ref} = 0 \quad (13f)$$

$$\mathbf{KG} \cdot \mathbf{P}_G + \mathbf{KL} \cdot \mathbf{PL} + \mathbf{KD} \cdot \tilde{\mathbf{L}}\mathbf{S} = \mathbf{KD} \cdot \mathbf{D} \quad (13g)$$

$$\tau_d^{Load} \leq CT_t + M \cdot \tilde{L}S_{dt}, \forall d, \forall t \quad (13h)$$

The restoration time in the energizing level is limited by delay which comes from the start-up characteristics function of an aggregated BS unit includes the start-up time of the traditional BS unit, DER units, and microgrids. This delay is dependent on the maximum available generation capacity of the BS units  $P_{gt, max}$  which is modeled as a piece-wise linear

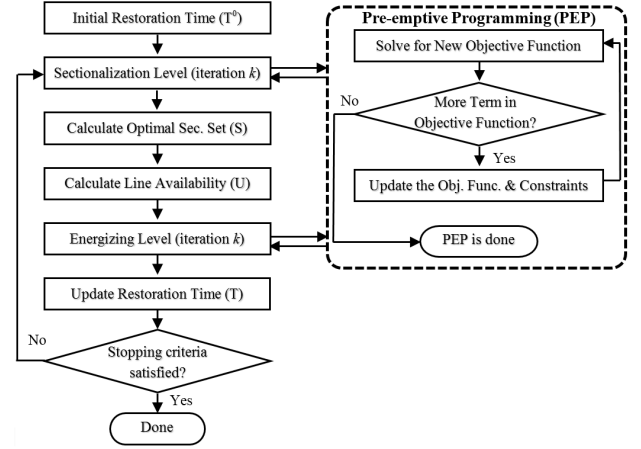


Fig. 5. Bi-level programming flowchart

function of time  $t$ :

$$P_{gt, max} = \begin{cases} 0, & t < T_{g\alpha} \\ RU_g \cdot (t - T_{g\alpha}), & T_{g\alpha} \leq t < T_{g\beta} \\ P_{g, max}, & t \geq T_{g\beta} \end{cases} \quad (14)$$

The ABS units with fast response capability of the DERs do not have the same cranking power process of NBS units. In (14), the available capacity ( $P_{gt, max}$ ) of an ABS unit cannot be negative as it was negative for the NBS units at warming up time. The ABS generation unit in our model switches at time zero,  $T_{g\alpha} = 0$ , when it begins to generate power. Then, depending on its ramp-up rate  $RU_g$ , it generates more power until its nominal maximum generation capacity at time  $T_{g\beta}$ .

The BLP flowchart is demonstrated at Fig. 5. Also, its algorithm has been elaborated, in Algorithm 1, in which demonstrates that after solving the sectionalization problem, the line availability  $\mathbf{U}$  and two indexes from resilience vector (1)  $\lambda_{AL}$  and  $\xi_{BTW}$  are determined in step 4 and 5.

---

#### Algorithm 1 The proposed bi-level programming algorithm

---

- 1: Initialize  $k$ ,  $\mathbf{T}$
  - 2: **while** not meeting the stopping criteria (8) **do**
  - 3:   Solve the sectionalization problem via PEP for  $\mathbf{S}^k$
  - 4:   Update  $\mathbf{U}^k$  based on  $\hat{\mathbf{S}}^k$ :  $U_l^k = \sum_{m=1}^{NBS} \hat{s}_{mb}^* \cdot \hat{s}_{m\acute{l}}^*$
  - 5:   Calculate  $\lambda_{AL}$  and  $\xi_{BTW}$
  - 6:   Solve the restoration problem via PEP for  $\tau^{k, Load}$
  - 7:   Calculate  $\tilde{\mathbf{T}}^k = \mathbf{KD} \cdot \tau^{k, Load}$
  - 8:   **for**  $b = 1, 2, \dots, NB$  **do**
  - 9:     **for**  $m = 1, 2, \dots, NBS$  **do**
  - 10:      **if**  $T_{mb}^{k-1} \geq \tilde{T}_b^k$  or  $T_{mb}^{k-1} = T_{mb}^0$  **then**
  - 11:        $T_{mb}^k = T_{mb}^o + s_{mb} \cdot \tilde{T}_b^k, \forall s_{mb} = 1$
  - 12:      **end if**
  - 13:     **end for**
  - 14:   **end for**
  - 15:   Calculate  $\Delta C_{LS}^R, \Delta C_T^R$ , and  $\Pi^R$
  - 16:    $k = k + 1$
  - 17: **end while**
-

## B. MPEC approach

There is also a close association between BLP and mathematical programming with equilibrium constraints (MPEC) approach. Both approaches are composed of two-level optimization models where the upper level's constraints region is embedded from the optimal solution of lower level [33]. The MPEC model of the power system restoration in this paper minimizes the objective function (15a) with respect to constraints (15b)-(15p), (9b)-(9g), (13g), and (13f), where  $\mathbf{e}_5 = [1]_{ND \times 1}$ ,  $\mathbf{E} = [1]_{ND \times NT}$ , and  $\boldsymbol{\mu}_i : i \in \{1, \dots, 9\}$  and  $\mathbf{v}_j : j = 1, 2$  are the dual variables. Hereby, the constraints (15b)-(15p), (13g), and (13f) are from the Karush-Kuhn-Tucker (KKT) conditions of the lower level model and (9b)-(9g) are the upper level original constraints.

$$\min_{\mathbf{s}, \mathbf{P}, \mathbf{L}, \mathbf{S}, \boldsymbol{\tau}} \quad \mathbf{w}^T \cdot \boldsymbol{\tau} \cdot \mathbf{e}_1 + VOLL \cdot \mathbf{e}_1^T \cdot \mathbf{L}\mathbf{S} \cdot \mathbf{e}_2 \quad (15a)$$

$$s.t. \quad \mathbf{C} \cdot \mathbf{e}_2^T + \mathbf{K}\mathbf{G}^T \cdot \mathbf{v}_1 + \boldsymbol{\mu}_1 - \boldsymbol{\mu}_2 + \Delta \boldsymbol{\mu}_3 - \Delta \boldsymbol{\mu}_4 = \mathbf{0} \quad (15b)$$

$$\mathbf{K}\mathbf{L}^T \cdot \mathbf{v}_1 + \boldsymbol{\mu}_5 - \boldsymbol{\mu}_6 + \boldsymbol{\mu}_7 - \boldsymbol{\mu}_8 = \mathbf{0} \quad (15c)$$

$$VOLL \cdot \mathbf{E} + \mathbf{K}\mathbf{D}^T \cdot \mathbf{v}_1 - M \cdot \boldsymbol{\mu}_9 = \mathbf{0} \quad (15d)$$

$$\boldsymbol{\omega} \cdot \mathbf{e}_2^T + \boldsymbol{\mu}_9 = \mathbf{0} \quad (15e)$$

$$\mathbf{K}\mathbf{G} \cdot \mathbf{v}_2 - \text{diag}^{-1}(\mathbf{x}) \cdot \mathbf{K}\mathbf{L}(\boldsymbol{\mu}_5 - \boldsymbol{\mu}_6) = \mathbf{0} \quad (15f)$$

$$\boldsymbol{\mu}_1^T \cdot (\mathbf{P}_G - \mathbf{P}_{G,max}) = \mathbf{0} \quad (15g)$$

$$\boldsymbol{\mu}_2^T \cdot (\mathbf{P}_{G,min} - \mathbf{P}_G) = \mathbf{0} \quad (15h)$$

$$\boldsymbol{\mu}_3^T \cdot (\Delta \mathbf{P}_G - \mathbf{U}\mathbf{R}) = \mathbf{0} \quad (15i)$$

$$\boldsymbol{\mu}_4^T \cdot (\mathbf{D}\mathbf{R} - \Delta \mathbf{P}_G) = \mathbf{0} \quad (15j)$$

$$\boldsymbol{\mu}_5^T \cdot (\mathbf{P}\mathbf{L} - \text{diag}^{-1}(\mathbf{x}) \cdot \Delta \boldsymbol{\theta} - M(\mathbf{e}_3 - \mathbf{U}) \cdot \mathbf{e}_2^T) = \mathbf{0} \quad (15k)$$

$$\boldsymbol{\mu}_6^T \cdot (-M(\mathbf{e}_3 - \mathbf{U}) \cdot \mathbf{e}_2^T - \mathbf{P}\mathbf{L} + \text{diag}^{-1}(\mathbf{x}) \cdot \Delta \boldsymbol{\theta}) = \mathbf{0} \quad (15l)$$

$$\boldsymbol{\mu}_7^T \cdot (\mathbf{P}\mathbf{L} - \mathbf{P}\mathbf{L}_{max}) = \mathbf{0} \quad (15m)$$

$$\boldsymbol{\mu}_8^T \cdot (-\mathbf{P}\mathbf{L}_{max} - \mathbf{P}\mathbf{L}) = \mathbf{0} \quad (15n)$$

$$\boldsymbol{\mu}_9^T \cdot (\mathbf{T}^{Load} \cdot \mathbf{e}_2^T - \mathbf{e}_5 \cdot \mathbf{C}\mathbf{T}^T - M \cdot \tilde{\mathbf{L}}\mathbf{S}) = \mathbf{0} \quad (15o)$$

$$\boldsymbol{\mu}_i \leq \mathbf{0}, \forall i \in \{1, \dots, 9\} \quad (15p)$$

## C. Pre-emptive goal programming

The proposed bi-level model has multiple terms in its objective function: restoration time, load shedding, and operation cost in both levels. We assume that the priority of these goals are known in advance. Hence, pre-emptive programming (PEP) is used to solve these models. PEP automatically takes care of the issue of different scales among these objective terms [38]. For example, given the order of priority in order as (1) to minimize load shedding, (2) to minimize restoration time, and (3) to minimize operation cost, one can follow the steps described below:

**Step 1 (a):** Solve optimization model (7) with a single objective function of minimizing load shedding, i.e.

$$\min VOLL \cdot \mathbf{e}_1^T \cdot \mathbf{L}\mathbf{S} \cdot \mathbf{e}_2$$

The optimal solution  $\mathbf{L}\mathbf{S}^*$  gives a theoretical lower bound on load shedding cost, i.e.,

$$VOLL \cdot \mathbf{e}_1^T \cdot \mathbf{L}\mathbf{S} \cdot \mathbf{e}_2 \geq VOLL \cdot \mathbf{e}_1^T \cdot \mathbf{L}\mathbf{S}^* \cdot \mathbf{e}_2.$$

**Step 1 (b):** Based on the result of Step 1(a), a new constraint (16) is constructed and added to optimization model (7):

$$VOLL \cdot \mathbf{e}_1^T \cdot \mathbf{L}\mathbf{S} \cdot \mathbf{e}_2 \leq VOLL \cdot \mathbf{e}_1^T \cdot \mathbf{L}\mathbf{S}^* \cdot \mathbf{e}_2 + \varepsilon_{l_s}, \quad \varepsilon_{l_s} \geq 0, \quad (16)$$

where,  $\varepsilon_{l_s}$  is an auxiliary variable to ensure feasibility of this newly added constraint in the next step. Similarly, these two steps are repeated for the second objective in sequence.

**Step 2 (a):**

$$\min \boldsymbol{\omega}^T \mathbf{T} + \kappa_{l_s} \cdot \varepsilon_{l_s}$$

**Step 2 (b):**

$$\boldsymbol{\omega}^T \mathbf{T} \leq \boldsymbol{\omega}^T \mathbf{T}^* + \varepsilon_t, \quad \varepsilon_t \geq 0 \quad (17)$$

**Step 3:** The last objective is defined to be the objective of the model (7) with newly added constraints (16) and (17):

$$\min \mathbf{c}^T \mathbf{P} \cdot \mathbf{e}_2 + \kappa_{l_s} \cdot \varepsilon_{l_s} + \kappa_t \cdot \varepsilon_t$$

**Step 4:** The final optimal value for the original objective function in the PEP algorithm is:

$$VOLL \cdot \mathbf{e}_1^T \cdot \mathbf{L}\mathbf{S}^* \cdot \mathbf{e}_2 + \boldsymbol{\omega}^T \mathbf{T}^* + \mathbf{c}^T \mathbf{P}^* \cdot \mathbf{e}_2 + \varepsilon_{l_s}^* + \varepsilon_t^*$$

## V. CASE STUDIES

Three case studies are designed to study model performance based on two factors: programming model and size of the network. Two programming models, including BLP and MPEC models, are presented in Section III, and two modified IEEE test systems consisting of 6-bus as a small scale and 118-bus as a large scale networks described in [40] are considered to illustrate the performance of the proposed restoration algorithm. In order to discuss the efficiency of the proposed approach in detail, this paper considers the following three cases:

**Case I:** The BLP model in small scale network.

**Case II:** The BLP model in large scale network.

**Case III:** The MPEC model in small and large scale grids.

These cases have been solved by using CPLEX 12.3.0.0 [41] under GAMS 24.4.5 [42] on a PC with Intel Xeon 2.53GHz, 12-core, and 128GB of RAM, to demonstrate the performance of the proposed resilience-based restoration; both models are solved over a daily time horizon.

Three BS generation units are utilized for the modified IEEE 6-bus test system located at buses 1, 2, and 6, and eight BS generation units are placed at buses 12, 25, 49, 59, 69, 80, 89, and 100 [10] in modified IEEE 118-bus test system. It is assumed that the proposed restoration and energizing strategy is applied after the cascading failure of an entire system, in a sense that all generation units and transmission lines are out of service or damaged after extreme event.

Generation units, demands, and branch input data are given in [40]. Table II prioritizes the power outage cost rate,  $w_b$ , of individual consumers at different sectors. For example, hospitals and data centers as critical consumers are defined in the "large users" sector with  $w_b$  equal to 1000 which shows the highest priority. To exhibit the performance of the model with respect to demand priority, all consumers are aggregated into three main categories of loads with the high, average, and low weights. In the next subsection, the corresponding numerical results are specified for each case study. It should be noted that the zero injection buses in the network (without generation units and loads) have the lowest priority with minimum value of outage cost rate,  $w_b$ .

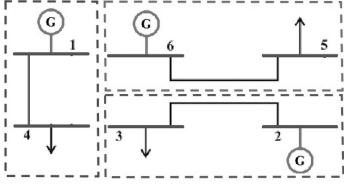


Fig. 6. Optimal sectionalized 6-bus IEEE test system

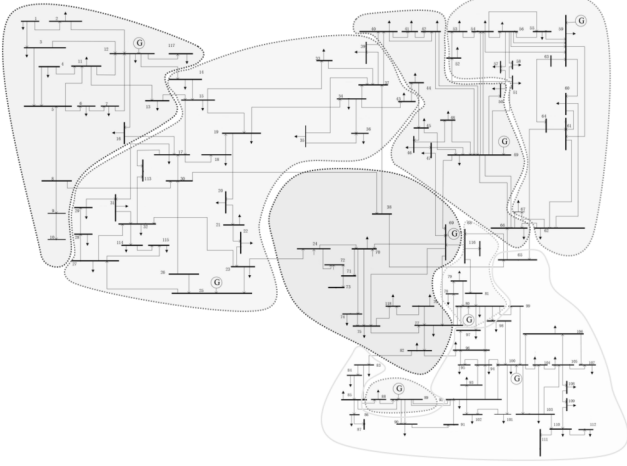


Fig. 7. 118-bus's sectionalized grid

#### A. Case I: The BLP model in small scale network

The BLP model (9) and (13) are implemented on a modified IEEE 6-bus test system. Figure 6 shows the optimal sectionalized power grid. Table I presents the optimal load shedding, restoration time, and the elements of resilience vector  $\mathfrak{R}$ .

Although the selected sectionalization is optimal for case I, there is 12% overall load shedding. In the first section, BS unit 1 has enough capacity to supply the load on bus 4, but line 1-4 limits the power flow to 100MW and causes 5% load shedding. In the second section, BS unit 2 and line 2-3 have enough capacity to provide the load on bus 3. In the last section, BS unit 3 and line 5-6 have lower capacity than the demanded load on bus 5 which leads to 26% unserved demand.

From a connectivity perspective, there are just two buses in each section. The obtained grid has the best value of 2 for algebraic connectivity ( $\lambda_{AL}$ ) because each load bus is supplied by one BS unit at each section, and there is no islanded load bus in the optimal solution. Betweenness centrality ( $\xi_{BTW}$ ) is equal to zero; upon its definition, no bus is located between any pair of buses within the sections. Since it is a small scale case, it is solved in one iteration, and the last resilience index  $\Pi^R$  is not applicable.

TABLE I  
CASE I AND II RESULTS VS. CASE III

Case	CPU time(s)	$LS^*$ (%)	$T^*$ (h)	Resilience vector ( $\mathfrak{R}$ )			
				$\Delta C_{LS}^R$ (\$M)	$\Delta C_T^R$ (\$K)	$\lambda_{AL}$	$\xi_{BTW}$
I	3.01	12.00	9.4	4.90	17.5	2	0
III-6bus	2.29	12.18	9.4	4.89	17.5	2	0
II	60.64	11.86	11.07	75.26	589	0.089	18.56
III-118bus	801.91	8.98	9.27	77.7	536	0.124	31.02

TABLE II  
CONSUMER OUTAGE COST RATE (\$/HR).

Category	Consumer Sector	w
High	Large users /Residential /Industrial	600-1000
Average	Commercial /Govt. & inst.	100-300
Low	Agricultural /Office & building	20-100

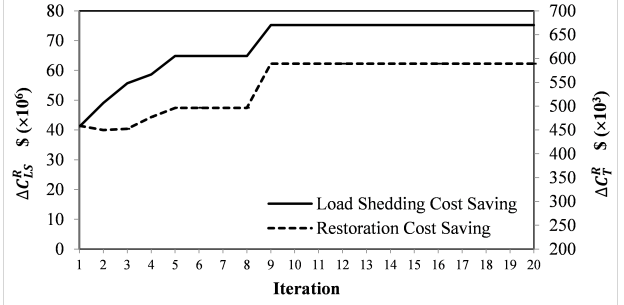


Fig. 8. Resilience indexes: Load shedding & restoration cost saving

#### B. Case II: the BLP in large scale network

The optimal sectionalized grid topology for case II is depicted at Fig. 7. The original grid is decomposed to eight sections. Figures 8, 9, 10, and 11 present the final restoration results for one run of the BLP algorithms on a large scale instance. To evaluate the sensitivity of the BLP algorithm in finding the optimal sections, the electrical loads are categorized to different levels within outage cost rate.

Figure 8 shows the trend of first and second resilience indexes at each iteration of BLP solution. These two indexes are raised dramatically due to restoration of most load buses, particularly all critical loads in high category. The load shedding cost saving ( $\Delta C_{LS}^R$ ) is settled down to \$505K from the initial iteration \$482K. The restoration cost saving ( $\Delta C_T^R$ ) is also increased by \$1700K.

Figure 9 presents the weighted algebraic connectivity ( $\lambda_{AL}$ ) and betweenness centrality ( $\xi_{BTW}$ ), third and fourth elements of resilience vector  $\mathfrak{R}$ . The transient behaviour at the beginning few iterations implies that the pattern of de-energized buses is changed among the sections. Hence, the grid has not been established yet and its connectivity is very low. After a while, the BLP finds the optimal place of the buses at each section where they are converged to the higher value at iteration 11. The minimum level of  $\lambda_{AL} = 0$  occurred at iteration 3 and 4, when 43% of lines got disconnected. Also, a pick value is observed for  $\xi_{BTW} = 42.21$  at iteration 2 while the values of  $\Delta C_{LS}^R$  and  $\Delta C_T^R$ , as presented in Fig. 8, are not high enough, and the cost of restoration time in Fig. 10 is on the maximum level \$419K, hence, this temporal peak value could not be an optimal value. Finally,  $\xi_{BTW}$  converged to 19 at iteration 11.

The last resilience index, adaptability ( $\Pi^R$ ) is also discussed. Adaptability with  $\alpha = 0.5$  is 36% which shows 36% improvement comparing initial iteration's results to the optimal result. Figure 10 shows some enhancement in cost of restoration after peak value in the cost of restoration curve at iteration 2 which is a smooth decline of the cost of restoration, from its maximum \$419K to \$368K at the final iteration 11.

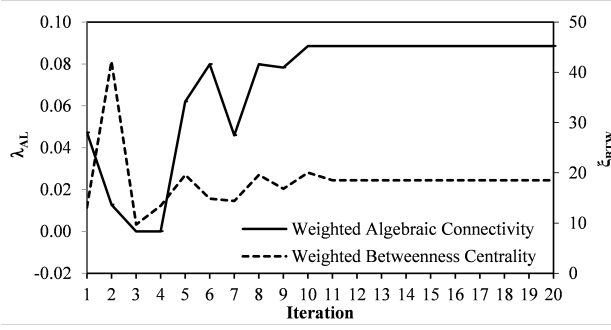


Fig. 9. Resilience indexes: Weighted algebraic connectivity & betweenness centrality

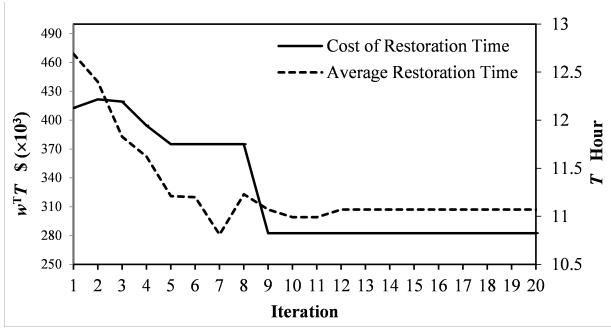


Fig. 10. Cost of restoration time and average restoration time

The average restoration time in Fig. 10 depicts a descending trend to the optimal restoration settling time of 11.05 hour.

Figure 11 presents the optimal restoration time of high to low consumer categories over iterations. At the first iteration, although all buses from high category restored within 11 hours, results show 15688MW and 28569MW load shedding in average and low category, respectively. As presented at iteration 2, these two categories energized faster than the first iteration while 1306MW load shedding happened in high category. Thereupon, the restoration times decreased until iteration 9 in which the optimal restoration time for all categories is obtained and no load shedding remained in high category loads. The sequences of optimal values of the load shedding and power generation cost in the energizing level are illustrated at Fig. 12. A 60% raise in generation cost is presented by Fig. 12 while load shedding cost is reduced by 60%; in view of the fact that, first, both are minimized in the objective function of the energizing model and, second, as the power generation marginal cost (C) is cheaper than the loss of load cost rate

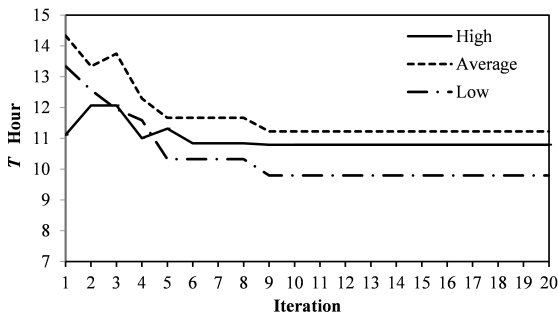


Fig. 11. Restoration time of high-average-low categories

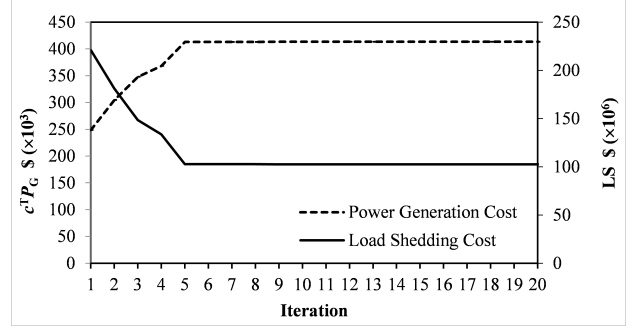


Fig. 12. Load shedding vs. power generation cost

value ( $VO_{LL}$ ), the cost of power generation is less than the load shedding cost curve.

### C. Case III: The MPEC model in small and large scale grids

Solving the developed MPEC model (15) for the small and large scale networks, gives the optimal solution for the problem. As presented in Table I, the MPEC solution methodology solved case I in 2.291 seconds which is almost the same as the BLP solved in 3.012 seconds. In case II, MPEC found the optimal solution in 13 minutes and 21.907 seconds while the BLP method solved the model in 1 minute and 2.518 seconds. Hence, the solutions of BLP are very close to MPEC and can be achieved faster in a large scale network.

From the results presented in the case studies, following observations can be made regarding these solution methods:

- BLP provides load shedding of 11.86% which is just 2.88% above MPEC that caused almost the same value of  $\Delta C_{LS}^R$  for both approaches. The restoration time achieved by BLP is 1.8 hours more than MPEC while  $\Delta C_T^R$  shows better value for BLP than MPEC. In view of this fact, BLP restored some loads in high category faster than MPEC. From connectivity perspective, MPEC gives a much more robust solution corresponding to a higher value in  $\lambda_{AL}$  and  $\xi_{BTW}$ .
- The BLP results were close enough to MPEC's results while it could solve the model faster than MPEC. Therefore, one can use the BLP if finding a sub-optimal solution fast is more important than the solution quality.

### D. Model effectiveness analysis

As explained in Section I, the power system restoration has been done through multiple approaches in the literature. Among these approaches two of the most relevant has been chosen: the first is [39] with ordered binary decision diagram (OBDD)-based system sectionalizing method and the second is [31] which has taken a minimum-tree-based approach. Their results for IEEE 118-bus test case have compared with the proposed resilience-based restoration's results in this paper in terms of two criteria, load shedding and restoration time. Note that, the assumptions about available BS units are different in these studies in comparison with the current paper. It is considered that the robustness metrics which are describing the connectivity of network's sections in restoration process have not been calculated in any of these two literature studies.

TABLE III  
COMPARISON ON THE RESTORATION METHODS FOR IEEE 118-BUS CASE

	OBDD	Minimum tree	BLP model
Total load shedding	54%	39.44%	11.86%
Average restoration time	N/A	14.18 h	11.07 h

Table III presents the OBDD method results in 54% load shedding which is much worse than the results of our proposed model and the restoration time was not provided in [39]. The second research work in [31] presents the restoration time of each section with the average of 14.18 hours, while by our proposed study, the restoration has been done within 11.07 hours. The load shedding amount by the minimum tree approach is also about 27% more than what is got in our BLP model by 11.86%. Therefore, in conclusion, the proposed methodology achieved better value in both load shedding and restoration time.

### E. Sensitivity analysis on resilience indexes

The proposed resilience vector encompasses five indexes. Two of these indexes, algebraic connectivity ( $\lambda_{AL}$ ) and betweenness centrality ( $\xi_{BTW}$ ) describes the robustness of the network while it is de-energized. In this section, a sensitivity analysis is performed to show how the power system performance could be influenced by these indexes. The other three indexes are direct functions of system's performance in terms of the load shedding and the restoration time.

The sensitivity of these robustness indexes is evaluated with respect to the amount of load shedding per iteration to capture the dependency of the robustness indexes and total served load at each section and each bus. These changes are described by two sensitivity indexes of  $S_{LS}^{\lambda}$  and  $S_{LS}^{\xi}$ .

$$S_{LS}^{\lambda} = \frac{\partial \bar{\lambda}_m}{\partial \bar{LS}_m} \quad (18)$$

$$S_{LS}^{\xi} = \frac{\partial \bar{\xi}_d}{\partial \bar{LS}_d} \quad (19)$$

Where,  $\bar{LS}_m$  and  $\bar{LS}_d$  are the summation of load shedding over the time, averaged per section and demand buses respectively as shown in (20) and (21). Since the results is available per iteration, the introduced sensitivity indexes are provided by discrete values of iterations ( $k$ ) as follows:

$$\bar{LS}_d = \frac{1}{ND} \sum_t^{NT} \sum_d^{ND} LS_{dt} \quad (20)$$

$$\bar{LS}_m = \frac{1}{NBS} \sum_t^{NT} \sum_d^{NBS} LS_{mt} \quad (21)$$

$$S_{LS}^{\lambda,k} = \left( \frac{\Delta \bar{\lambda}_m}{\Delta \bar{LS}_m} \right)^k = \frac{\bar{\lambda}_m^{k+1} - \bar{\lambda}_m^k}{\bar{LS}_m^{k+1} - \bar{LS}_m^k} \quad (22)$$

$$S_{LS}^{\xi,k} = \left( \frac{\Delta \bar{\xi}_d}{\Delta \bar{LS}_d} \right)^k = \frac{\bar{\xi}_d^{k+1} - \bar{\xi}_d^k}{\bar{LS}_d^{k+1} - \bar{LS}_d^k} \quad (23)$$

Where,  $\bar{\lambda}_m^k$  is the average of algebraic connectivity of the sections at iteration  $k$ . The average of Betweenness centrality of buses with demand on them at iteration  $k$  is presented by  $\bar{\xi}_d^k$ . The average of sections' load shedding and demands' load shedding are also shown by  $\bar{LS}_m^k$  and  $\bar{LS}_d^k$  respectively per section. The proposed indexes are determined following Algorithm 2.

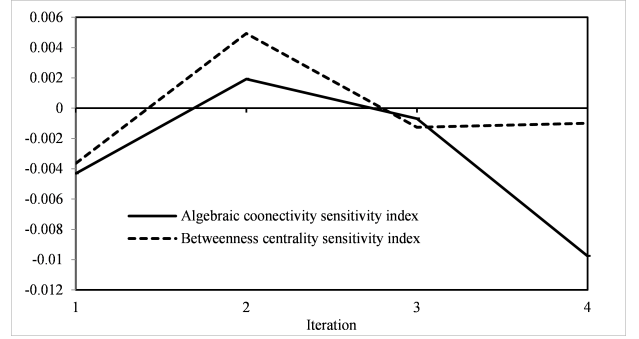


Fig. 13. Algebraic connectivity and betweenness centrality vs. load shedding

Figure 13 shows the changes of sensitivity indexes over iterations for the large-scale case of IEEE 118-bus test system. As demonstrated in most of the iterations, it gets a negative value which indicates that effect of algebraic connectivity and betweenness centrality on load shedding is decreasing. In optimal iteration, minimum value of load shedding implies the maximum level of algebraic connectivity and betweenness centrality.

### Algorithm 2 The sensitivity indexes calculation

- 1: Initialize  $k$ ,  $\mathbf{T}$
- 2: Solve the BLP model at the first iteration and update  $\mathbf{T}$
- 3: **while** not meeting the stopping criteria (8) **do**
- 4:     Solve the BLP model and update  $\mathbf{T}$
- 5:     Determine  $S_{LS}^{\lambda,k}$  and  $S_{LS}^{\xi,k}$
- 6:      $k = k + 1$
- 7: **end while**

## VI. CONCLUSION

In this work, the problem on power system restoration was considered after complete blackout, targeting the maximum resilience. The problem was solved by sectionalizing the network and penetrating one BS unit per section. A BLP model with linear sectionalization constraints caused lower complexity and faster convergence than a single-level model. Such a problem was solved with the pre-emptive programming approach. Through two case-studies based on the 6-bus and 118-bus IEEE, the sequence of optimality shows 15% and 200% elevation on load shedding and restoration cost savings. Further comparison with the MPEC equivalence of the problem, was presented near the global optimality of the solution by the numerical results. Additionally, in the sensitivity analysis, the performance of robustness indexes were discovered by varying the load shedding at each iteration for buses and sections. Future research can be completed on this topic, from different perspectives such as considering uncertainties on loads, or vulnerability of the grid under imposed shocks. The proposed model can provide an emergency restoration to any de-energized transmission network with a few simple modifications.

## REFERENCES

- [1] Y. Liu and C. Singh, "A methodology for evaluation of hurricane impact on composite power system reliability." *IEEE Transactions on Power Systems*, vol. 26, no. 1, pp 145-152, 2011.

- [2] Y. Liu and C. Singh, "Evaluation of Hurricane Impact on Failure Rate of Transmission Lines Using Fuzzy Expert System." *Intelligent System Applications to Power Systems*, ISAP'09. 15th International Conference on. IEEE, 2009.
- [3] R. Berg, "Hurricane Ike (AL092008) 114 September 2008." *National Hurricane Center Tropical Cyclone Rep*, 2009.
- [4] G. Li, P. Zhang, P. B. Luh, W. Li, Z. Bie, C. Serna and Z. Zhao, "Risk analysis for distribution systems in the northeast US under wind storms." *IEEE Transactions on Power Systems*, vol 29, no 2, pp 889-898, 2014.
- [5] M. Panteli, P. Mancarella, S. Wilkinson, R. Dawson, and C. Pickering, "Assessment of the resilience of transmission networks to extreme wind events." In *PowerTech*, 2015 IEEE Eindhoven, pp. 1-6. IEEE, June 2015.
- [6] S. Chanda, and A.K. Srivastava, "Quantifying resiliency of smart power distribution systems with distributed energy resources." in *Industrial Electronics (ISIE)*, 2015 IEEE 24th International Symposium, 2015.
- [7] C. Middlebrook, V. Ranganathan, and N. N. Schulz, "A case study on blackout restoration as an educational tool". *IEEE Transactions on Power Systems*, 15(2), 467-471, 2000.
- [8] M. M. Adibi, and L. H. Fink. "Power system restoration planning." *IEEE Transactions on Power Systems* 9.1: 22-28. 1994.
- [9] T. Nagata, and H. Sasaki, "A multi-agent approach to power system restoration." *IEEE Transactions on power systems*, 17(2), 457-462, 2002.
- [10] S. A. N. Sarmadi, A. S. Dobakhshari, S. Azizi, and A. M. Ranjbar, "A sectionalizing method in power system restoration based on WAMS." *IEEE Transactions on Smart Grid*, 2(1), 190-197, 2011.
- [11] J. N. Jiang, Z. Zhang, M. Fan, G. Harrison, C. Lin, M. Tamayo, and V. Perumalla, "Power system restoration planning and some key issues." In 2012 IEEE Power and Energy Society General Meeting (pp. 1-8). IEEE. July 2012.
- [12] J. Q. Torts, and V. Terzija, "A smart power system restoration based on the merger of two different strategies." In 2012 3rd IEEE PES Innovative Smart Grid Technologies Europe (ISGT Europe) (pp. 1-8). IEEE, Oct 2012.
- [13] M. Chaudry, P. Ekins, K. Ramachandran, A. Shakoor, J. Skea, G. Strbac, X. Wang, and J. Whitaker, "Building a resilient UK energy system." 2011.
- [14] A.R. Berkeley III, M. Wallace, and C. COO, "A framework for establishing critical infrastructure resilience goals." Final Report and Recommendations by the Council, National Infrastructure Advisory Council, 2010.
- [15] M. Panteli and P. Mancarella, "The grid: Stronger, bigger, smarter?: Presenting a conceptual framework of power system resilience." *IEEE Power and Energy Magazine*, 13(3): 58-66, 2015.
- [16] L. H. Fink and K. Carlsen, "Operating under Stress and Strain." *IEEE Spectrum*, March 1978, pp. 48-53.
- [17] Y. Lu, C.Y. Chang, W. Zhang, L.D. Marinovici, and A.J. Conejo, "On Resilience Analysis and Quantification for Wide-Area Control of Power Systems." arXiv preprint arXiv:1604.05369, 2016.
- [18] M. Ouyang, and Z. Wang, "Resilience assessment of interdependent infrastructure systems: With a focus on joint restoration modeling and analysis." *Reliability Engineering & System Safety*, 141, pp.74-82, 2015.
- [19] M. Panteli, P. Mancarella, D. Trakas, E. Kyriakides, and N. Hatziargyriou, "Metrics and Quantification of Operational and Infrastructure Resilience in Power Systems." *IEEE Transactions on Power Systems*, 2017.
- [20] M. Ouyang, and L. Dueas-Osorio, "Multi-dimensional hurricane resilience assessment of electric power systems." *Structural Safety*, 48, pp.15-24, 2014.
- [21] M. Fiedler, "Algebraic connectivity of graphs." *Czechoslovak mathematical journal*, 23(2): p. 298-305, 1973, 2014.
- [22] L.C. Freeman, "A set of measures of centrality based on betweenness." *Sociometry*: p. 35-41. 1977.
- [23] A. Bigdeli, A. Tizghadam, and A. Leon-Garcia. "Comparison of network criticality, algebraic connectivity, and other graph metrics." in *Proceedings of the 1st Annual Workshop on Simplifying Complex Network for Practitioners*. ACM, 2009.
- [24] L.J.A. Peas, C.L.F. Moreira, and O. Resende, "Control strategies for microgrids black start and islanded operation." *Int. J. Distr. Energy Resources*, 2, pp.211-231, 2006.
- [25] L. H. Fink, K. L. Liou, and C. C. Liu, "From generic restoration actions to specific restoration strategies." *IEEE Transactions on power systems*, 10(2), 745-752, 1995.
- [26] F.F. Wu, and A. Monticelli, "Analytical tools for power system restoration-conceptual design." *IEEE Transactions on Power Systems*, 3(1), 10-26, 1988.
- [27] J. Quirs-Torts, M. Panteli, P. Wall, and V. Terzija, "Sectionalizing methodology for parallel system restoration based on graph theory." *IET Generation, Transmission and Distribution*, 9(11), 1216-1225, 2015.
- [28] W. Liu, Z. Lin, F. Wen, C. Y. Chung, Y. Xue, G. Ledwich, "Sectionalizing strategies for minimizing outage durations of critical loads in parallel power system restoration with bi-level programming." *International Journal of Electrical Power & Energy Systems*, 71, 327-334, 2015.
- [29] W.P. Luan, M.R. Irving, and J.S. Daniel, "Genetic algorithm for supply restoration and optimal load shedding in power system distribution networks." *IEE Proceedings-Generation, Transmission and Distribution*, 149(2), pp.145-151, 2002.
- [30] S. Toune, H. Fudo, T. Genji, Y. Fukuyama, and Y. Nakanishi, "Comparative study of modern heuristic algorithms to service restoration in distribution systems." *IEEE Transactions on Power Delivery*, 17(1), pp.173-181, 2002.
- [31] C. Li, J. He, P. Zhang, and Y. Xu, "A Novel Sectionalizing Method for Power System Parallel Restoration Based on Minimum Spanning Tree." *Energy*, 10(7), p.948, 2017.
- [32] L. Sun, C. Zhang, Z. Lin, F. Wen, Y. Xue, M.A. Salam, and S.P. Ang, "Network partitioning strategy for parallel power system restoration." *IET Generation, Transmission & Distribution*, 10(8), pp.1883-1892, 2016.
- [33] E. Cotilla-Sanchez, P. D. Hines, C. Barrows, S. Blumsack, and M. Patel, "Multi-attribute partitioning of power networks based on electrical distance." *IEEE Transactions on Power Systems*, 28(4), 4979-4987, 2013.
- [34] W. Liu, Z. Lin, F. Wen, and G. Ledwich, "A wide area monitoring system based load restoration method." *IEEE Transactions on Power Systems*, 28(2), 2025-2034, 2013.
- [35] A. Sydney, C. Scoglio, and D. Gruenbacher, "Optimizing algebraic connectivity by edge rewiring." *Applied Mathematics and computation*, 219(10): p. 5465-5479, 2013.
- [36] A. N. Sadigh, M. Mozafari, and B. Karimi, "Manufacturerretailer supply chain coordination: A bi-level programming approach." *Advances in Engineering Software*, 45(1), 144-152, 2012.
- [37] F. Glover, "Improved linear integer programming formulations of non-linear integer problems." *Management Science*, 22(4), 455-460, 1975.
- [38] J. P. Ignizio, "Goal programming and extensions." Lexington Books, 1976.
- [39] C. Wang, V. Vittal, and K. Sun, "OBDD-based sectionalizing strategies for parallel power system restoration." *IEEE Transactions on Power Systems*, 26(3), pp.1426-1433, 2011.
- [40] "A Parallel Sectionalized Restoration Scheme for Resilient Smart Grid Systems - Data Set" [Online], Available: <http://e2map.egr.uh.edu/publications>.
- [41] The ILOG CPLEX, 2008. [Online]. Available: <http://www.ilog.com/products/cplex/>.
- [42] R. E. Rosenthal, GAMS: A Users Guide, GAMS Development Corporation, Washington, Sep. 2016.



**Saeedeh Abbasi** is a Ph.D. candidate in the Industrial Engineering Department at the University of Houston. Her research interests include mathematical modeling, robust optimization, smart grid system, and network resiliency.



**Masoud Barati** received a Ph.D. degree in Electrical Engineering from Illinois Institute of Technology, Chicago. Presently, he is an assistant professor in the Electrical and Computer Engineering Department at Louisiana State University, Baton Rouge, LA. His research interests include microgrid operation and planning, microeconomics, mathematical modeling and multiple infrastructure assessment.



**Gino J. Lim** is a professor and chair of industrial engineering, and Hari and Anjali Faculty Fellow at the University of Houston. He holds a Ph.D. in Industrial Engineering from University of Wisconsin-Madison. His research interest lies in developing optimization techniques for solving large scale decision making problems in areas such as network resiliency, supply chain under disruption and transportation networks. His current research includes robust optimization in transportation problems, smart ports, and scheduling.